Formation of naked singularities in five-dimensional space-time

Yuta Yamada[1,*] and Hisa-aki Shinkai[1,2,†]

[1]*Faculty of Information Science and Technology, Osaka Institute of Technology,*
1-79-1 Kitayama, Hirakata, Osaka 573-0196, Japan
[2]*Computational Astrophysics Laboratory, Institute of Physical and Chemical Research (RIKEN),*
Hirosawa, Wako, Saitama 351-0198, Japan

We numerically investigate the gravitational collapse of collisionless particles in spheroidal configurations both in four- and five-dimensional (5D) space-time. We repeat the simulation performed by Shapiro and Teukolsky (1991) that announced an appearance of a naked singularity, and also find similar results in the 5D version. That is, in a collapse of a highly prolate spindle, the Kretschmann invariant blows up outside the matter and no apparent horizon forms. We also find that the collapses in 5D proceed more rapidly than in 4D, and the critical prolateness for the appearance of an apparent horizon in 5D is loosened, compared to 4D cases. We also show how collapses differ with spatial symmetries comparing 5D evolutions in single-axisymmetry, SO(3), and those in double-axisymmetry, U(1) $\times$ U(1).

I. INTRODUCTION

The so-called "large extra-dimensional models" as a consequence of brane-world pictures have changed our viewpoints for a way of understanding the fundamental forces. The scenarios of unifying the gravity at TeV scale or so open the possibility of verification of higher-dimensional space-time models at the CERN LHC. If the LHC detects productions (and evaporations) of mini black holes as expected, then humankind will encounter a Copernican change of our outlook of the Universe.

With this background, black holes in higher-dimensional space-time have been extensively studied for a decade. Many interesting discoveries of new solutions have been reported, and their properties are being revealed. However, fully relativistic dynamical features, such as the formation processes, stabilities and late-time fate, are still unknown and they are waiting to be studied. Several groups, including us, have begun reporting numerical studies in various topics in higher-dimensional models [1–6].

In this article, we report our numerical simulations on gravitational collapse in axisymmetric space-time. The topic has been studied in many ways in (3 + 1)-dimensional space-time (4D, hereafter); among them, we think the most impressive result is the work by Shapiro and Teukolsky [7] (ST91, hereafter); a highly prolate matter collapse, which may form a naked singularity. We repeat their simulations and also compare them with (4 + 1)-dimensional (5D) versions.

In classical general relativity, it is well known that a space-time singularity will be generally formed in the gravitational collapse of nonsingular asymptotically flat initial data. If a singularity forms without an event horizon,

all physical predictions become invalid. In order to avoid such a disastrous situation, Penrose proposed the *cosmic censorship conjecture* [8], which states that singularities are always clothed by event horizons.

On the other hand, for nonspherical gravitational collapses, Thorne proposed the *hoop conjecture* [9] which states that black holes with horizons are formed when and only when a mass gets compacted into a small region. He expressed the compactness with a *"hoop"* around matter. If matter configuration is highly aspherical, then the hoop length becomes larger. If so, the conjectured inequality does not hold, i.e. a horizon will not be formed. Thereby, the hoop conjecture indicates that a highly aspherical matter collapse will lead to a naked singularity.

ST91 numerically showed that axisymmetric space-time with collisionless matter particles in spheroidal distribution will collapse to singularity, and there are no apparent horizons formed when the spheroids are highly prolate. The behaviors are consistent with their initial data analysis [10], and support the hoop conjecture. However, since numerical evolutions cannot provide the final structures nor the conclusive information for formation of naked singularities, debates were raised after their announcement. For example, Wald *et al* [11,12] showed examples that 3-dimensional hypersurfaces can hit singularities; nevertheless, the space-time is consistent with cosmic censor. Their examples are not directly related to the numerical results with ST91, but we learned that a numerical result provides only limited evidence.

Regarding the 5D cases, the hoop conjecture is supposed to be replaced with the *hyper-hoop* version [13–17], in which the criterion is not a hoop but a surface. In our previous work [1], we numerically constructed initial data sequences of nonrotating matter for 5D evolutions and examined the hyper-hoop conjecture using minimum *area* around the matter. We found that the areal criterion

*[*]yamada@is.oit.ac.jp
[†]shinkai@is.oit.ac.jp

matches with the appearance of apparent horizons for spindle matter configurations, but not for ring configurations. The sequences suggest that a highly prolate spindle in 5D will form a naked singularity similar to the 4D cases. We also found that the condition for a naked singularity formation is more relaxed in 5D than in 4D cases.

One of the objectives of the present work is to compare the dynamics between 4D and 5D. A simple estimation from the free-falling time indicates that the gravitational collapse in 5D takes longer than in 4D cases. We show this is not applicable to the highly nonlinear final stages. In 5D, two axes can be settled as rotational symmetric axes, so that we also compare gravitational collapses in axisymmetry with those in "doubly"-axisymmetric space-time.

II. NUMERICAL CODE

We evolve five-dimensional axisymmetric (symmetric on z-axis, SO(3)) or doubly-axisymmetric [symmetric both on x and z-axes, U(1) × U(1)], asymptotically flat space-time (see Fig. 1). For the comparison, we also performed four-dimensional axisymmetric space-time evolutions.

We start our simulation from time symmetric and conformally flat initial data, which are obtained by solving the Hamiltonian constraint equations [1]. The asymptotical flatness is imposed throughout the evolution, which settles the fall-off condition to the metric as $\sim 1/r$ for 4D cases and $\sim 1/r^2$ for 5D cases.

The matter is described with 5000 collisionless particles, which move along the geodesic equations. We smooth out the matter by expressing each particle with a Gaussian density distribution function, with its typical width twice as much as the numerical grid. The particles are homogeneously distributed in a spheroidal shape, parametrized with a and b (Fig. 1), or eccentricity $e = \sqrt{1 - a^2/b^2}$.

By imposing axisymmetry or double-axisymmetry, our model becomes practically a $(2 + 1)$-dimensional problem. We construct our numerical grids with the Cartesian coordinate (x, z), and apply the so-called Cartoon method [2,18] to recover the symmetry of space-time.

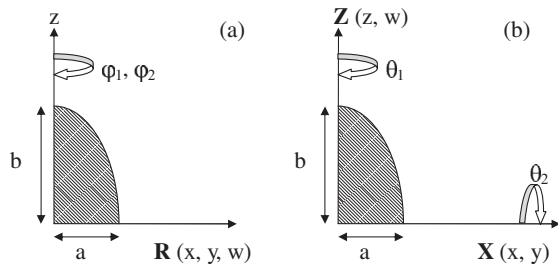The space-time is evolved using the Arnowitt-Deser-Misner (ADM) evolution equations. It is known that the

ADM evolution equations excite an unstable mode (constraint-violation mode) in long-term simulations [19,20]. However, we are free from this problem, since gravitational collapse occurs within quite a short time. By monitoring the violation of constraint equations during evolutions, we confirm that our numerical code has second-order convergence, and also that the simulation continues in stable manner. The results shown in this report are obtained with numerical grids, $129 \times 129 \times 2 \times 2$. We confirmed that higher resolution runs do not change the physical results.

We use the maximal slicing condition for the lapse function α, and the minimal strain condition for the shift vectors β^i. Both conditions are proposed for avoiding the singularity in numerical evolutions [21], and the behavior of α and β^i roughly indicates the strength of gravity, conversely. The iterative Crank-Nicolson method is used
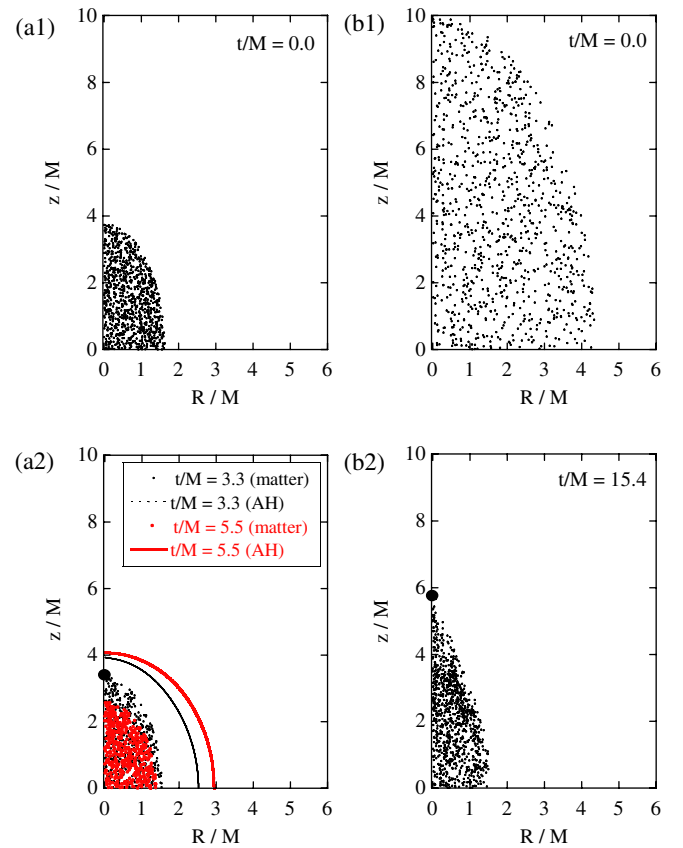

FIG. 2 (color online). Snapshots of 5D axisymmetric evolution with the initial matter distribution of $b/M = 4$ [(a1) and (a2); model $5\text{DS}\beta$ in Table I] and 10 [(b1) and (b2); model $5\text{DS}\delta$]. We see the apparent horizon (AH) is formed at the coordinate time $t/M = 3.3$ for the former model and the area of AH increases, while AH is not observed for the latter model up to the time $t/M = 15.4$, when our code stops due to the large curvature. The big circle indicates the location of the maximum Kretschmann invariant $I_{\max}$ at the final time at each evolution. Number of particles are reduced to $1/10$ for figures.

FIG. 1. We evolve five-dimensional (a) axisymmetric [SO(3)] or (b) double-axisymmetric [U(1) × U(1)], asymptotically flat space-time using the Cartesian grid. The initial matter configuration is expressed with parameters a and b.

for integrating ADM evolution equations, and the Runge-Kutta method is used for matter evolution equations.

For discussing physics, we search the location of apparent horizon (AH) and calculate the Kretschmann invariant ($I = R_{abcd}R^{abcd}$) on the spatial hypersurface.

III. RESULTS

We prepare several initial data fixing the total ADM mass and the eccentricity of distribution, $e = 0.9$. By changing the initial matter distribution sizes, we observe the different final structures. Figure 2 shows snapshots of 5D axisymmetric evolutions of model $b/M = 4$ and 10 (model $5DS\beta$ and $5DS\delta$, respectively; see Table I); the former collapses to a black hole while the latter collapses without AH formation.

All the models we tried result in forming a singularity (i.e., diverging I). We stopped our numerical evolutions when the shift vector was not obtained with sufficient accuracy due to the large curvature. For model $5DS\delta$, we integrated up to the coordinate time $t/M = 15.4$ and the maximum of the Kretschmann invariant I_{max} became $O(1000)$ on z axis (see Fig. 3), but AH was not formed.

When the initial matter is highly prolate, AH is not observed. This is consistent with 4D cases [7,10], and matches with the predictions from initial data analysis in 5D cases [1,14]. The location of I_{max} is on z-axis, and just outside of the matter [22]. This is again the same with 4D cases [7]. The absence of AH with diverging I suggests a formation of naked singularity in 5D.

In order to compare the results with 4D and 5D, we reproduced the results of ST91. We then find that the $e = 0.9$ initial data with $b/M = 10$ (model $4D\delta$) collapses without forming AH, and the code stops at the coordinate time $t = 20.91$ with $I_{max} = 84.3$ on the z-axis ($z/M = 6.1$); all the numbers match quite well with ST91.
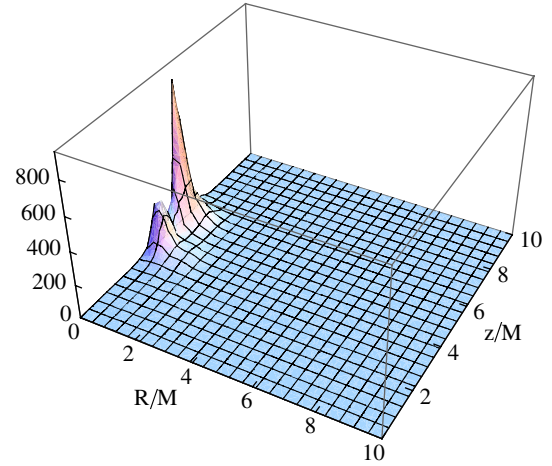

FIG. 3 (color online). Kretschmann invariant I for model $5DS\delta$ at $t/M = 15.4$. The maximum is $O(1000)$, and its location is on z-axis, just outside of the matter.

(Note that our slicing conditions and coordinate structure are not the same as in ST91.)

Figure 4 compares hypersurfaces for the 5D models which collapse (a) with forming AH, (b) without forming AH, and (c) 4D collapses without forming AH. We see hypersurfaces are bending due to the slicing conditions, and figures tell us how numerically integrated region covers the space-time.

We also performed 5D collapses with doubly-axisymmetric [U(1) × U(1)] space-time. The matter and space-time evolve quite similarly to the 5D and 4D axisymmetric cases, but we find that the critical configurations for forming AH are different. Table I summarizes the main results of 4D and two 5D cases. We find that AH in 5D is formed in larger b initial data than 4D cases. This result is consistent with our prediction from the sequence of initial

TABLE I. Model names and the results of their evolutions whether we observed AH or not. The eccentricity e of the collapsed matter configurations is also shown; e_{AH} and e_f are at the time of AH formation (if formed), and on the numerically obtained final hypersurface, respectively.

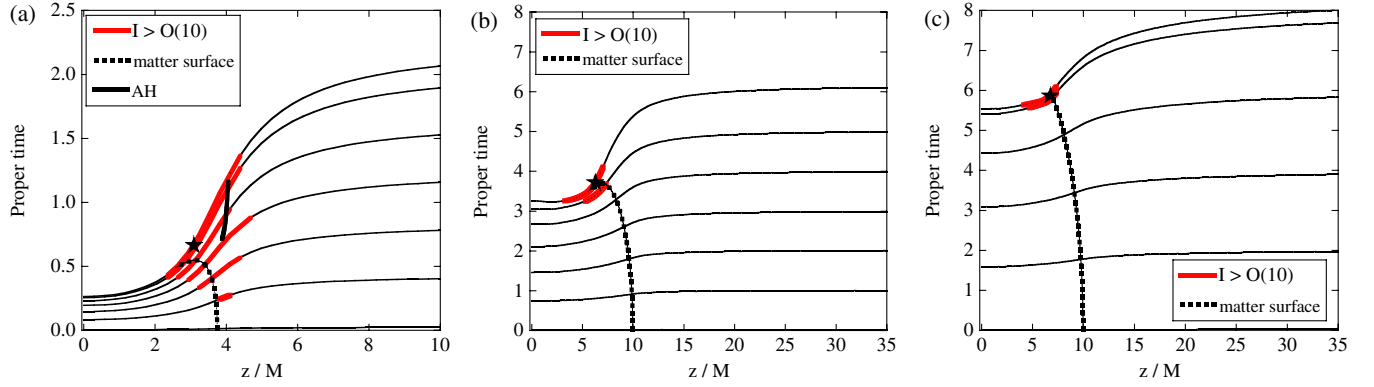| $b/M(t = 0)$	2.50	4.00	6.25	10.00
4D axisym.	$4D\alpha$	$4D\beta$	$4D\gamma$	$4D\delta$
	AH-formed	no	no	no
	$e_{AH} = 0.90$			
	$e_f = 0.92$	$e_f = 0.89$	$e_f = 0.92$	$e_f = 0.96$
5D axisym.	$5DS\alpha$	$5DS\beta$	$5DS\gamma$	$5DS\delta$
SO(3)	AH-formed	AH-formed	no	no
	$e_{AH} = 0.88$	$e_{AH} = 0.88$		
	$e_f = 0.82$	$e_f = 0.84$	$e_f = 0.88$	$e_f = 0.96$
5D double	$5DU\alpha$	$5DU\beta$	$5DU\gamma$	$5DU\delta$
axisym.	AH-formed	AH-formed	AH-formed	no
U(1) × U(1)	$e_{AH} = 0.86$	$e_{AH} = 0.87$	$e_{AH} = 0.92$	
	$e_f = 0.79$	$e_f = 0.81$	$e_f = 0.90$	$e_f = 0.98$

FIG. 4 (color online).   The snapshots of the hypersurfaces on the z axis in the propertime versus coordinate diagram; (a) model $5DS\beta$, (b) model $5DS\delta$, and (c) model $4D\delta$. The uppermost hypersurface is the final data in numerical evolution. We also mark the matter surface and the location of AH if exist. The ranges with $\mathcal{I} \geq 10$ are marked with bold lines and peak value of $\mathcal{I}$ expressed by asterisks.

data [1]. AH criteria with initial b are loosened for 5D doubly-axisymmetric cases.

We also show the eccentricity of matter, e_{AH} and e_f, at the time of AH formation (if formed) and at the final time in the simulation, respectively. The numbers in Table I indicate that the eccentricity itself is not a guiding measure for AH formation, but they giveus a hint for understanding the differences.

In 4D, the eccentricity increases after AH is formed ($4D\alpha$), while it decreases in 5D axisymmetric cases ($5DS\alpha$ and $5DS\beta$). That is, the 5D collapses proceed towards spherical configurations. This fact would be explained by the degree of freedom of the movements. In general, 5D space-time is expected to produce much more gravitational radiation than 4D space-time [3,5], since more modes of oscillation exist. Gravitational radiation normally works to change shapes to spherical, because it is produced from the acceleration of space-time and carries the energy away. (It is known that a compact binary system

FIG. 5 (color online).   The Kretschmann invariant $\mathcal{I}$ at the location of $\mathcal{I}_{max}$ on the final hypersurface is plotted as a function of proper time at its location. Labels indicate model names in Table I. The time of AH formation ($t = 0.6$ for model $5DS\beta$, $t = 0.9$ for $5DU\beta$) is shown by a dot.

will evolve into a circular orbit due to the emission of gravitational radiation.) Therefore, collapses in 5D space-time are likely to evolve towards more spherical. This interpretation together with the hoop conjecture will explain why the AH-formation condition is loosened in 5D cases.

In the 5D doubly-axisymmetric cases, on the other hand, the magnitude of e_f is smaller than 5D axisymmetric cases for small b/M cases ($5DS\alpha$ vs $5DU\alpha$, or $5DS\beta$ vs $5DU\beta$), while it is larger for large b/M cases ($5DS\gamma$ vs $5DU\gamma$, or $5DS\delta$ vs $5DU\delta$). We think this is because the doubly-axisymmetric collapses proceed in a more symmetric manner than axisymmetric collapse near the origin, while they proceed in more 4D-like axisymmetric collapses near the axes far from the origin. The collapses of small b/M initial data, therefore, will evolve into a more spherical shape, while the large b/M initial data will evolve, increasing the eccentricity, where the latter is similar to 4D cases.

In Fig. 5, we plot $\mathcal{I}$ at the point which gives $\mathcal{I}_{max}$ on the final hypersurface as a function of proper time. The $\mathcal{I}$ diverges at the end of simulations in all the cases, but the diverging time becomes later for larger b/M initial data. We see that 5D collapses are generally proceeding more rapidly than 4D collapses. We also see that collapses in 5D doubly-axisymmetric space-time is proceeding more slowly than 5D single-axisymmetric cases. If we observe further, the model $5DU\beta$ evolves quite similarly to $5DS\beta$, while $5DU\delta$ evolves quite similarly to $4D\delta$. These behaviors support the previous understandings of the evolution of the eccentricity.
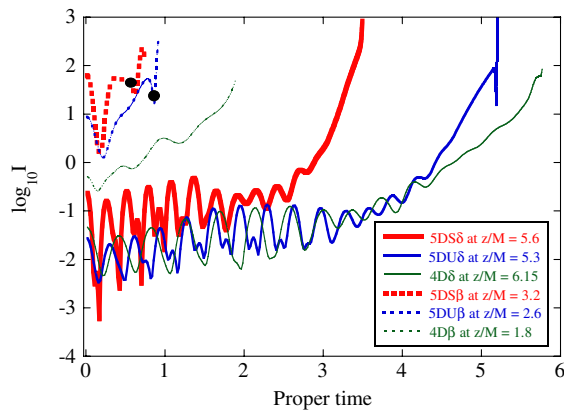
IV. DISCUSSIONS

In this article, we reported our numerical study of gravitational collapses in 5D space-time. We collapsed spheroidal matter expressing with collisionless particles, and observed the evolution of the Kretschmann invariant and the apparent horizon (AH) formation.

The collapsing behaviors are generally quite similar to the cases in 4D, but we also found that (a) 5D-collapses proceed rapidly than 4D-collapses, (b) AH appears in more highly prolate matter configurations than 4D cases, (c) doubly-axisymmetric [U(1) × U(1)] assumption makes collapse proceed towards more spherical when it forms AH, but presents quite similar behavior with 4D cases for large configurations, and (d) the positive evidence for appearance of a naked singularity in 5D.

Up to this moment, we only checked the existence of apparent horizons, and not the event horizons. The system does not include any angular momentum. We are implementing our code to cover these studies.

We are now preparing our next detailed report including the validity of the hyper-hoop conjecture in 5D, and the cases of the ring objects.

ACKNOWLEDGMENTS

[1] Y. Yamada and H. Shinkai, Classical Quantum Gravity **27**, 045012 (2010).
[2] H. Yoshino and M. Shibata, Phys. Rev. D **80**, 084025 (2009).
[3] M. Shibata and H. Yoshino, Phys. Rev. D **81**, 021501 (2010); **81**, 104035 (2010).
[4] M. Zilhão *et al.*, Phys. Rev. D **81**, 084052 (2010).
[5] H. Witek *et al.*, Phys. Rev. D **82**, 104014 (2010).
[6] L. Lehner and F. Pretorius, Phys. Rev. Lett. **105**, 101102 (2010).
[7] S. L. Shapiro and S. A. Teukolsky, Phys. Rev. Lett. **66**, 994 (1991).
[8] R. Penrose, Riv. Nuovo Cimento Soc. Ital. Fis. **1**, 252 (1969).
[9] K. S. Thorne, in *Magic Without Magic*, edited by J. R. Klauder (Freeman, San. Francisco, 1972), p. 231.
[10] T. Nakamura, S. L. Shapiro, and S. A. Teukolsky, Phys. Rev. D **38**, 2972 (1988).
[11] R. M. Wald and V. Iyer, Phys. Rev. D **44**, R3719 (1991).
[12] M. A. Pelath, K. P. Tod, and R. M. Wald, Classical Quantum Gravity **15** 3917 (1998).
[13] D. Ida and K. Nakao, Phys. Rev. D **66**, 064026 (2002).
[14] C-M. Yoo, K. Nakao, and D. Ida, Phys. Rev. D **71**, 104014 (2005).
[15] C. Barrabés, V. P. Frolov, and E. Lesigne, Phys. Rev. D **69**, 101501 (2004).
[16] J. M. M. Senovilla, Europhys. Lett. **81**, 20004 (2008).
[17] G. W. Gibbons, arXiv:0903.1580.
[18] M. Alcubierre *et al.*, Int. J. Mod. Phys. D **10**, 273 (2001).
[19] see e.g., H. Shinkai, J. Korean Phys. Soc. **54**, 2513 (2009).
[20] H. Shinkai and G. Yoneda, Gen. Relativ. Gravit. **36**, 1931 (2004).
[21] L. Smarr and J. W. York, Jr., Phys. Rev. D **17**, 2529 (1978).
[22] The Kretschmann invariant expresses the strength of the curvature, which is determined by the gradient of metric. For example, when we solve a single star with uniform density, the maximum value of the metric appears at the center of matter configuration, but the maximum value of the metric gradient appears off center and likely at the outside of matter region. Therefore, our results for the location of the maximum Kretschmann invariant is not so odd.